Explaining and Validating Stressed Power Systems Behavior Using Modal Series

Naser Pariz, Hasan Modir Shanechi, *Senior Member, IEEE*, and Ebrahim Vaahedi, *Fellow, IEEE*

***Abstract*—In this paper, qualitative and quantitative differences between nonlinear and linear modal simulations in stressed power system are presented. For the first time in the literature, time-domain nonlinear simulation is used to validate the accuracy of the second order modal model, obtained by using modal series. Furthermore three new selective indices are defined and used to explain and predict the differences between nonlinear and linear modal simulations. These indices also explain the under or over damping results being experienced when a linear system theory designed controller is applied to a nonlinear system.**

***Index Terms*—Modal interaction, modal series, normal forms of vector fields, stressed power system, system security.**

I. Introduction

When a stressed power system is subjected to a disturbance, it exhibits complex dynamic behavior. The complexity of this behavior depends on the power system structure, system loading, and type and location of the disturbance. For example the inter-area mode phenomenon in stressed power systems and auto and hetero parametric resonance in power systems can be addressed to some of these complex behaviors [1], [2].

A. Prologue

Two approaches are commonly used to study the power system dynamic behavior. One is nonlinear simulation and the other is linear modal analysis. It is difficult to understand and gain a good feeling for the physical nature of the complex dynamic behavior (of stressed power system) by nonlinear simulation. On the other hand, the validity of linear modal analysis is restricted to a small neighborhood of the operating point and therefore, when a system is subjected to large disturbances and its states are driven away from operating point, the similarity between real time responses and linear modal simulation is lost.

Recently, the technique of normal forms of vector fields has been used to analyze the complex behavior of the power systems [3]–[6]. In this paper a new method, called Modal Series Method [7], [8], is used to show, validate and explain the qualitative and quantitative differences between nonlinear and linear modal simulation, in stressed power systems. These differences are negligible in relaxed power systems.

Manuscript received February 26, 2001; revised June 5, 2002.

N. Pariz is with the Department of Electrical Engineering, Ferdowsi University, Mashhad, 9177948944-1111, Iran (e-mail: n-pariz@ferdowsi.um.ac.ir).

H. M. Shanechi is now with the Department of Electrical Engineering, New Mexico Tech, Socorro, NM 87801 USA. He was with the Electrical Engineering Department of Ferdowsi University, Mashad, Iran (e-mail: shanechi@ee.nmt.edu).

E. Vaahedi is with Perot Systems, Dallas, TX 75075 USA (e-mail: ebrahim.vaahedi@ps.net).

Digital Object Identifier 10.1109/TPWRS.2003.811307

It is shown that some oscillation frequencies may appear in stressed power systems which are not predictable by linear modal analysis. This qualitative difference is clarified by means of the discrete Fourier transform, and its physical nature is explained, using second order modal analysis, obtained via Modal Series. Also a comparison between nonlinear and second order modal simulation results is made. It is shown that these results agree with a good degree of approximation. These have been lacking in the literature.

B. Modal Interaction

It is well known that when a linear system is excited in steady state mode by a sinusoidal input, all system states have the same frequencies as the frequencies present in the input. This is not true when the system is nonlinear. For example when a static quadratic system is excited by sum of two sinusoidal inputs with frequencies ω_1 and ω_2, one can see a DC component and AC components with frequencies, $\omega_1, 2\omega_1, \omega_2, 2\omega_2$ and $\omega_1 \pm \omega_2$ at the output, whereas with linear systems, only the frequencies ω_1 and ω_2 are observed at the output.

In nonlinear dynamical system this behavior is more complicated. Suppose $\lambda_1, \lambda_2, \ldots, \lambda_N$ are linear modes of a nonlinear dynamical system. Because of the nonlinearity in system dynamics, these linear modes interact and produce many interaction modes of the form $m_1\lambda_1 + m_2\lambda_2 + \cdots + m_N\lambda_N$, where $m_i \in I$ and $i = 1, 2, \ldots, N$. The degree of the excitation of these modes, in zero input response, depends on nonlinearities and initial conditions. In this paper the authors show these interaction modes in stressed power system response. A closed form approximate solution, based on linear modes, is needed to understand and analyze the effects of modal interaction. Second order modal approximate solution, using Modal Series, is used for this purpose in this paper. Even higher order modal approximate solution is needed when an observed behavior cannot be explained using second order modal approximation. Our method would work as well with higher order approximations similarly to what is presented here for the second order.

II. Modal Series

A. Introduction

By using Modal Series it is possible to represent nonlinear dynamic systems, as well as stressed power systems, in a manner which yields a good deal of physical insight into the problem under consideration. Moreover, the method of solution has the great conceptual advantage of presenting a nonlinear system as a rather straightforward generalization of the linear case, although it may be much more involved. As with the normal form technique, this method is restricted to polynomial nonlinearity therefore, the Taylor series of other nonlinearity types are needed. Moreover, this method provides closed form solution to the differential equations even in the face of resonance condition.

B. Taylor Series Expansion

Let in an n generator system the dynamical equations governing the generators and their excitation systems have the general form:

$$\dot{X} = F(X) \tag{1}$$

where, $X = \left[\omega_1, E'_{q1}, E'_{d1}, X_{E1}, X'_{E1}, E_{fd1}, \ldots\right]^T$ is the state vector and $F: R^N \to R^N$ is a smooth vector field. Let the total order of the system (1) be N. Expanding (1) as Taylor series about a stable equilibrium point X_{SEP} and using again X and x_i as the new state variables yields;

$$\dot{x}_i = A_i X + \frac{1}{2} X^T H^i X + H.O.T. \tag{2}$$

where, it is assumed that X belongs to the convergence domain of the Taylor series $\upsilon \subseteq R^N$, A_i is the ith row of Jacobian matrix A which is equal to $[\partial F_i/\partial X]_{X_{\mathrm{SEP}}}$, and $H^i = [\partial^2 F_i/\partial x_k \partial x_l]_{X_{\mathrm{SEP}}}$ is the Hessian Matrix.

C. Eigenvalue Analysis and Jordan Form of the System

Denote by Λ the (complex) Jordan form of A and by U and V the matrices of the right and left eigenvectors respectively. Then the transformation $X = UY$ yields the following equivalent system for (2)

$$\dot{y}_j = \lambda_j y_j + \sum_{k=1}^{N}\sum_{l=1}^{N} C_{kl}^j y_k y_l \tag{3}$$

where,

$$C^j = \frac{1}{2}\sum_{p=1}^{N} V_{jp}^T [U^T H^p U] = \left[C_{kl}^j\right] \tag{4}$$

and V_{jp}^T is the j-th element of the p-th column of V^T.

D. Modal Series

Let us decompose the solution of (3) for initial conditions, $Y_o = [y_{1o}, \ldots, y_{No}]^T$, as

$$y_j(t) = y_{1j}(t) + y_{2j}(t) + y_{3j}(t) + \cdots \tag{5}$$

where, $y_{mj}(t)$ contains the terms that depends on any m-statess multiples of initial conditions. For example for $m = 3$, y_{3j} contains the terms that depend on any combination such as $(y_{po} y_{qo} y_{ro})$ for $p, q, r = 1, \ldots, N$. Since (5) must satisfy (3):

$$\begin{aligned}\dot{y}_{1j} + \dot{y}_{2j} + \dot{y}_{3j} + \cdots =& \lambda_j (y_{1j} + y_{2j} + y_{3j} + \cdots)\\ &+ \sum_{k=1}^{N}\sum_{l=1}^{N} C_{kl}^j\\ &\times (y_{1k} + y_{2k} + y_{3k} + \cdots)\\ &\times (y_{1l} + y_{2l} + y_{3l} + \cdots) + \cdots \end{aligned} \tag{6}$$

The solution of (6) can be found by solving the following differential equations with initial condition $y_{1j}(0) = y_{j0}$ and $y_{mj}(0) = 0$ for $m \succ 1$ [7], [8]:

$$\begin{cases} \dot{y}_{1j} = \lambda_j y_{1j} & \text{(6-1)}\\ \dot{y}_{2j} = \lambda_j y_{2j} + \sum_{k=1}^{N}\sum_{l=1}^{N} C_{kl}^j y_{1k} y_{1l} & \text{(6-2)}\\ \dot{y}_{3j} = \lambda_j y_{3j} + \sum_{k=1}^{N}\sum_{l=1}^{N} C_{kl}^j (y_{1k} y_{2l} + y_{2k} y_{1l}) & \text{(6-3)}\\ \vdots \end{cases}$$

Equation (6-1) yields linear approximate solution to the system, its Laplace transform and time domain solution are given in (6-1-1) and (6-1-2) respectively.

$$Y_{1j}(s) = \frac{y_{j0}}{s - \lambda_j} \tag{6-1-1}$$

$$y_{1j}(t) = y_{j0} e^{\lambda_j t} \tag{6-1-2}$$

Equation (6-2) yields correction terms to linear approximate solution by considering second order nonlinearity. It can be solved by two dimensions Laplace transform [7]

$$Y_{2j}(s_1, s_2) = \sum_{k=1}^{N}\sum_{l=1}^{N} \frac{1}{(s_1 + s_2 - \lambda_j)} C_{kl}^j Y_{1k}(s_1) Y_{1l}(s_2). \tag{6-2-1}$$

To obtain the time domain solution, inverse transform of (6-2-1) can be calculated as:

$$y_{2j}(t) = \sum_{k=1}^{N}\sum_{l=1}^{N} C_{kl}^j S_{kl}^j(t) \tag{6-2-2}$$

where

$$S_{kl}^j(t) = \frac{y_{k0} y_{l0}}{\lambda_k + \lambda_l - \lambda_j}\left(e^{(\lambda_k + \lambda_l)t} - e^{\lambda_j t}\right) \text{ for } (k, l, j) \in R_2 \tag{6-2-3-a}$$

$$S_{kl}^j(t) = y_{k0} y_{l0} t e^{\lambda_j t} \text{ for } (k, l, j) \in R_2 \tag{6-2-3-b}$$

The set R_2 contains all three tuples (k, l, j), which cause the second order resonance condition, i.e., satisfy $\lambda_k + \lambda_l = \lambda_j$. Similar procedure may be carried out to calculate $y_{3j}(t)$ and higher order terms. Let us call the condition $|\lambda_k + \lambda_l - \lambda_j| \le 0.001\,|\lambda_j|$ second order quasiresonance and denote by R'_2 the set of all three tuples (k, l, j), which cause the second order quasiresonance. Neglecting $y_{3j}(t)$ and higher order terms, $y_j(t)$ and $x_i(t)$ can be approximated by:

$$\begin{aligned} y_j(t) =& y_{1j}(t) + y_{2j}(t)\\ =& \left(y_{j0} - \left\{\sum_{k=1}^{N}\sum_{l=1}^{N} h2_{kl}^j y_{k0} y_{l0}\right\}_{(k,l,j)\notin R'_2}\right) e^{\lambda_j t}\\ &+ \left\{\sum_{k=1}^{N}\sum_{l=1}^{N} h2_{kl}^j y_{k0} y_{l0} e^{(\lambda_k + \lambda_l)t}\right\}_{(k,l,j)\notin R'_2}\\ &+ \left\{\left(\sum_{k=1}^{N}\sum_{l=1}^{N} c_{kl}^j y_{k0} y_{l0}\right) t e^{\lambda_j t}\right\}_{(k,l,j)\in R'_2} \end{aligned} \tag{7}$$

$$
\begin{aligned}
x_i(t) = &\sum_{j=1}^{N} u_{ij} \left(y_{j0} - \left\{ \sum_{k=1}^{N}\sum_{l=1}^{N} h2_{kl}^{j} y_{k0} y_{l0} \right\}_{(k,l,j)\notin R_2'} \right) \\
&\times e^{\lambda_j t} \\
&+ \left\{ \sum_{j=1}^{N}\sum_{k=1}^{N}\sum_{l=1}^{N} u_{ij} h2_{kl}^{j} y_{k0} y_{l0} e^{(\lambda_k+\lambda_l)t} \right\}_{(k,l,j)\notin R_2'} \\
&+ \left\{ \sum_{j=1}^{N} \left(\sum_{k=1}^{N}\sum_{l=1}^{N} u_{ij} c_{kl}^{j} y_{k0} y_{l0} \right) t e^{\lambda_j t} \right\}_{(k,l,j)\in R_2'}
\end{aligned} \tag{8}
$$

where $h2_{kl}^{j} = C_{kl}^{j}/(\lambda_k + \lambda_l - \lambda_j)$.

Rearranging second order modal effects i.e., the second term in (8)

$$
\begin{aligned}
&\sum_{j=1}^{N} u_{ij} \left[\sum_{k=1}^{N}\sum_{l=1}^{N} h_{2kl}^{j} y_{k0} y_{l0} e^{(\lambda_k+\lambda_l)t} \right]_{(k,l,j)\notin R_2'} \\
&\quad = \sum_{k=1}^{N}\sum_{l=1}^{N} \left(y_{k0} y_{l0} \sum_{j=1}^{N} u_{ij} h_{2kl}^{j} \right)_{(k,l,j)\notin R_2'} e^{(\lambda_k+\lambda_l)t}
\end{aligned} \tag{9}
$$

and defining new constants L_j^i, K_{kl}^i and M_j^i as:

$$
L_j^i \triangleq u_{ij} \left(y_{j0} - \left\{ \sum_{k=1}^{N}\sum_{l=1}^{N} h2_{kl}^{j} y_{k0} y_{l0} \right\}_{(k,l,j)\notin R_2'} \right) \tag{10}
$$

$$
K_{kl}^i \triangleq y_{k0} y_{l0} \sum_{j\in J_{kl}} u_{ij} h2_{kl}^{j} \tag{11}
$$

where,

$$
J_{kl} = \{ j | (k,l,j) \notin R_2' \}
$$

$$
M_j^i \triangleq \sum_{k=1}^{N}\sum_{l=1}^{N} u_{ij} c_{kl}^{j} y_{k0} y_{l0} \text{ for } (k,l,j) \in R_2' \tag{12}
$$

the second order approximate response becomes:

$$
\begin{aligned}
x_i(t) &= \sum_{j=1}^{N} L_j^i e^{\lambda_j t} + \sum_{j=1}^{N} M_j^i t e^{\lambda_j t} + \sum_{k=1}^{N}\sum_{l=1}^{N} K_{kl}^i e^{(\lambda_k+\lambda_l)t} \\
&= \sum_{j=1}^{N} (L_j^i + M_j^i t) e^{\lambda_j t} + \sum_{k=1}^{N}\sum_{l=1}^{N} K_{kl}^i e^{(\lambda_k+\lambda_l)t}
\end{aligned} \tag{13}
$$

It is well known that linear modal analysis gives $x_i(t)$ as:

$$
x_i(t) = \sum_{j=1}^{N} u_{ij} y_{j0} e^{\lambda_j t} \tag{14}
$$

Similarly to (7) and (8) in this paper, (7) and (8) in [4] provide another approximation to $y_j(t)$ and $x_i(t)$ using normal forms of vector fields method. There are three differences between the two methods:

- The coefficients of these equations in [4] depend on Z_0 which has nonlinear relation to X_0, but in this paper they depend on Y_0 which has linear relation to X_0.
- The calculation of these coefficients, in case of resonance or quasiresonance, in the method in [4] is not as straight forward as it is here.
- Most importantly, Modal Series Method provides a more accurate approximation of the nonlinear system than the normal form technique in that second order Modal Series approximation captures more of the effects of nonlinearity than second order normal form approximation [7], [8].

III. Nonlinear Interactions

By comparing (13) and (14), two differences can be seen. One of them is the third term in (13) which gives an explicit correction term to linear approximate solution. It contains the second order modes i.e., $e^{(\lambda_k+\lambda_l)t}$ for all pairs λ_k and λ_l, $(k,l,j) \notin R_2'$. The other is the difference between linear approximate solution and the first two terms of (13). This difference indicates that the linear modes can be modulated by time, in case of resonance, and/or be excited or relaxed by higher order nonlinearity effects. By using (13) one can extend linear participation factors concept to include second-order modes [9].

IV. Second Order Modal Interactions Indices

The second order modal time response term, $K_{kl}^i e^{(\lambda_k+\lambda_l)t}$, is affected by two parameters. The absolute value of the constant K_{kl}^i determines the maximum (at time zero) amplitude. The larger this value, the more pronounced the effect of this interacting second order mode will be. The time constant of this second order mode, $\tau_{kl} = -1/\mathrm{real}(\lambda_k + \lambda_l)$, determines how fast this response vanishes. The larger this time constant is, the longer the effect of this mode will persist. Therefore, $I2_{kl}^i$, the product of the two, is defined as a measure for the effects of the interaction modes in the time response to capture both the amplitude and the duration effects of the interacting modes

$$
I2_{kl}^i = \left| \frac{K_{kl}^i}{\mathrm{real}(\lambda_k + \lambda_l)} \right| \quad i = 1, \ldots, N \tag{15}
$$

Also, to analyze the time modulation and/or the excitation or relaxation effects of the nonlinearity on linear modes, the following measures are used:

$$
MI_j^i = \left| \frac{M_j^i}{\mathrm{real}(\lambda_j)} \right| \tag{16}
$$

$$
I1_j^i = \frac{\mathrm{sign}\,(|u_{ij} y_{j0}| - \delta) \cdot |L_j^i|}{\max(\delta, |u_{ij} y_{j0}|)} \quad i = 1, \ldots, N \tag{17}
$$

The maximum of envelope of the mode $te^{\lambda_j t}$ in the second term of (13) is $|2e^{-1} M_j^i / \mathrm{real}(\lambda_j)|$, therefore MI_j^i is selected as the measure of the impact of this component. This is the component that captures the effect of all resonating second order modes. Note that the envelope of $te^{\lambda_j t}$ reaches its maximum at time $T_{\max} = -1/\mathrm{real}(\lambda_j)$, therefore its maximum may be large but it may not appear in simulation time and therefore its effects go unnoticed in simulation results.

In linear modal analysis the excitation level of mode $e^{\lambda_j t}$ in state i is given by $|u_{ij} y_{j0}|$. This excitation level is modified and changed to $\left|L_j^i\right|$ by nonlinearity effects as is evident in the first term of (8) and (13). A natural measure to assess the influence of the nonlinearity would be $\left|L_j^i\right| / |u_{ij} y_{j0}|$. The drawback for this choice is that when $|u_{ij} y_{j0}|$ is very small this quotient will be very large, even for small values of $\left|L_j^i\right|$, indicating that the nonlinearity has modified the effect of mode j in state i greatly. This means that we will have a large measure but, because of the small value of $\left|L_j^i\right|$, not a very pronounced effect. To compensate for these cases the measure $I1_j^i$ is defined. $I1_j^i$ approximates the actual excitation level of each linear mode with respect to that obtained via linear analysis, when its sign is positive, i.e., $|u_{ij} y_{j0}|$ is not very small. It denotes the excitation level with respect to δ when its sign is negative, i.e., in cases that $|u_{ij} y_{j0}|$ is very small. δ is a properly small positive number such as 0.1 $\max_j(|u_{ij} y_{j0}|)$, in this paper it is chosen to be 0.1. Therefore when $I1_j^i$ is close to one, it means that the excitation level of linear mode j is not changed considerably by the nonlinearity, or even if it has changed it is still not very pronounced in the state i.

V. Nonlinear Interaction Identification Procedure

Based on the above indices, the following algorithm is presented for the identification of modal interaction.

1. For a given disturbance, the states X_{cl} at the end of the disturbance are determined using nonlinear time domain simulation.
2. The post disturbance stable equilibrium point X_{SEP} of the system is determined.
3. The Taylor series expansion of the system around X_{SEP} is obtained.
4. Using similarity transformation from the eigen analysis of the linear part of Taylor series, second order approximate system is obtained in the Y variable.
5. The initial condition $X_0 = X_{cl} - X_{\mathrm{SEP}}$ is transformed to Y_0 using $Y_0 = U^{-1} X_0$ and the modal series analysis is done.
6. For each i, N^2 indices using **(15)** are calculated and compared to obtain dominant second order modes.
7. For each i, N indices using **(16)** are calculated to determine the modulated excitation effects of the nonlinearity.
8. For each i, N indices using **(17)** are calculated to identify the level of the nonlinear excitation of each linear mode with respect to that obtained via linear analysis or to δ.
9. Using the results of step 6, 7 and 8 we can predict or explain the differences between linear modal simulation and nonlinear simulation.

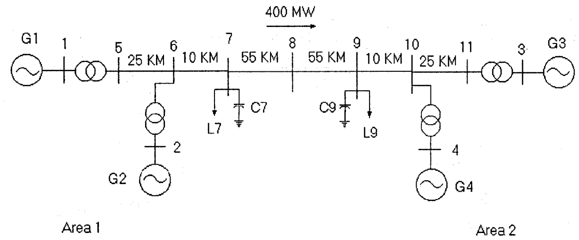

Fig. 1. Two-area four-machine test system.

TABLE I
Mechanical Modes of the Two-Area, 4-Generator Power System

	Without PSS	With PSS on Gen. 1	
λ_1, λ_2	0.12629 ± 3.39470I (0.5403 Hz)	-0.07222 ± 3.4774I (0.5534 Hz)	Inter-area Mode
λ_3, λ_4	-0.39090 ± 6.6499I (1.0584 Hz)	-0.38903 ± 6.6945I (1.0655 Hz)	Area-1 Local Mode Gen. 1 and 2
λ_5, λ_6	-0.38859 ± 6.6989I (1.0662 Hz)	-1.5618 ± 5.7489I (0.9150 Hz)	Area-2 Local Mode Gen. 3 and 4
λ_7	-0.00012	-0.000012	Zero Mode

VI. Numerical Examples

A. Two-Area, 4-Generator Power System

1) Description: Two-area four-generator power system ([10 in Section 12.8]) shown in Fig. 1 is used to show the differences between linear modal simulation and nonlinear simulation. Quasi steady state parameters and constant impedance models are used to represent the network and loads respectively. All generators are represented by two-axis model equipped with static exciters. The system parameters, load conditions and exciter data can be found in [8]. For 0.4 second we open the line between buses 7 and 8 and then close it to simulate a fault. Increasing the fault on time to 0.45 second made the system unstable.

2) Eigenvalues: This system has 27 eigenvalues without PSS; 14 representing 7 complex conjugate pairs and 13 real eigenvalues. Mechanical modes are listed in Table I. As we see in this table, the uncompensated system has negatively damped inter-area mode with frequency 3.3947 rad /sec (0.54 Hz), and has two positively damped local modes with frequencies 6.6499, 6.6989 rad/sec (1.058, 1.066 Hz). A classical PSS is designed in the frequency range (0.01, 2) Hz and placed on generator 1, its parameters are given in [7]. New mechanical modes are listed in Table I.

3) Difference between Linear Modal and Nonlinear Simulation Results: The original nonlinear system and the linear modal approximate system were simulated to show the qualitative differences between nonlinear system and its linear modal approximation. Some of the results are shown in Fig. 2. There are considerable differences between the two simulation results. Although both trajectories have the same initial state, the response of the linear system is damped oscillatory around zero, whereas the nonlinear response is a damped oscillatory

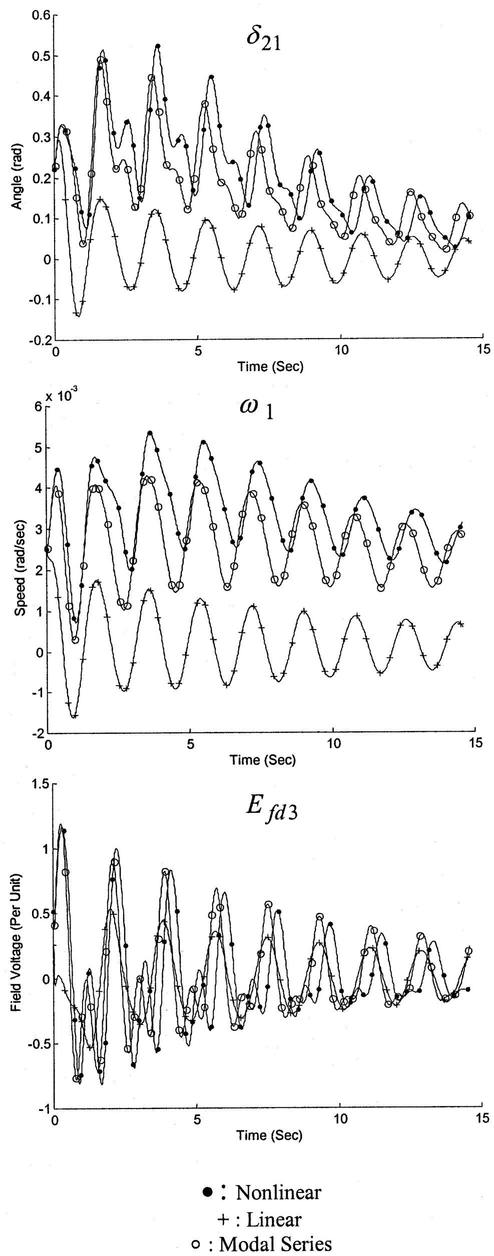

Fig. 2. Nonlinear, linear and second order modal series simulation results.

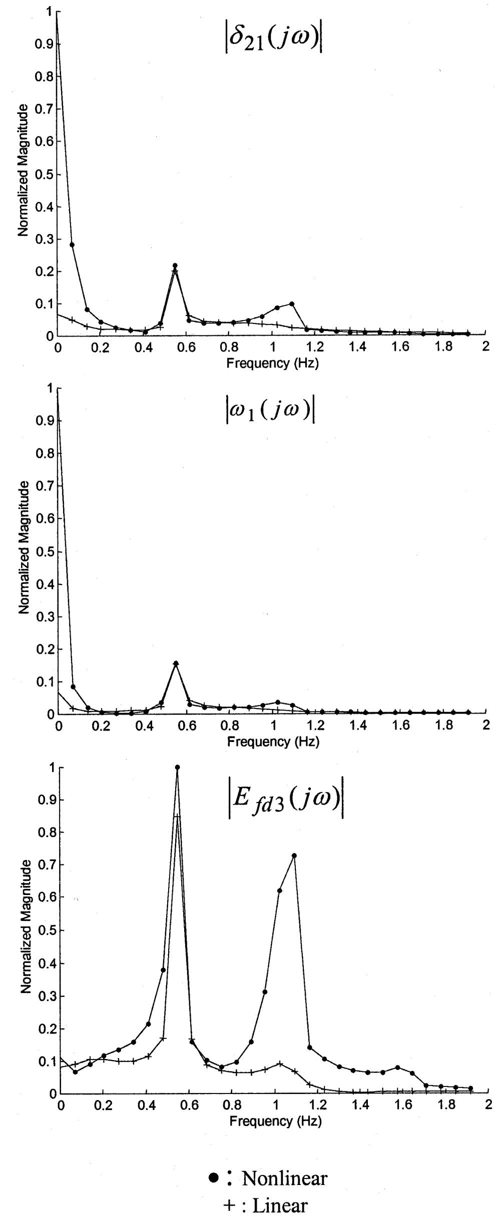

Fig. 3. Nonlinear, linear modal FFT's.

around an exponentially decaying bias. The origins of these differences are discussed in Section VII.

4) Similarity between Second Order Modal and Nonlinear Simulation: Using (8), second order modal simulation results were obtained and are shown in Fig. 2. The results show the good correspondence between nonlinear and second order modal simulation. Therefore, (8) can be used to explain the mechanism that causes the differences between nonlinear and linear modal simulation.

5) Identifying the Second Order Modal Interaction Frequency Using DFT: We see two oscillation frequencies in nonlinear simulation results, one of them being dominant. Linear simulation results show only one oscillation frequency. DFT was used to identify these frequencies. Please see Fig. 3. The DFT of the nonlinear system response shows that there are two oscillation frequencies, one of them is about 0.55 Hz (this is inter-area mode which is dominant) and the other is about 1.1 Hz. Is the later frequency from second order modal interaction or is it the local mode frequency of the area 1? If it were the local mode frequency, the nonlinearity effects must have excited it, because it is not seen in linear system responses and their DFT's. But $I1_j^i$ for this local mode, area-2 local mode, and inter-area mode are respectively about 1.17, -0.05 and -0.8 for δ_{2l} and 1.09, 1.2 and -0.7 for E_{fd3}, i.e., the nonlinearity effects do not change the local and the two inter-area mode excitation levels considerably. Therefore it is concluded that this is the frequency of one of the second order interaction modes.

6) Predicting Nonlinear Interaction between Modes: Compensated system has 30 eigenvalues. These 30 eigenvalues interact with each other and produce many second order modes. In other words, in the nonlinear system response, besides the

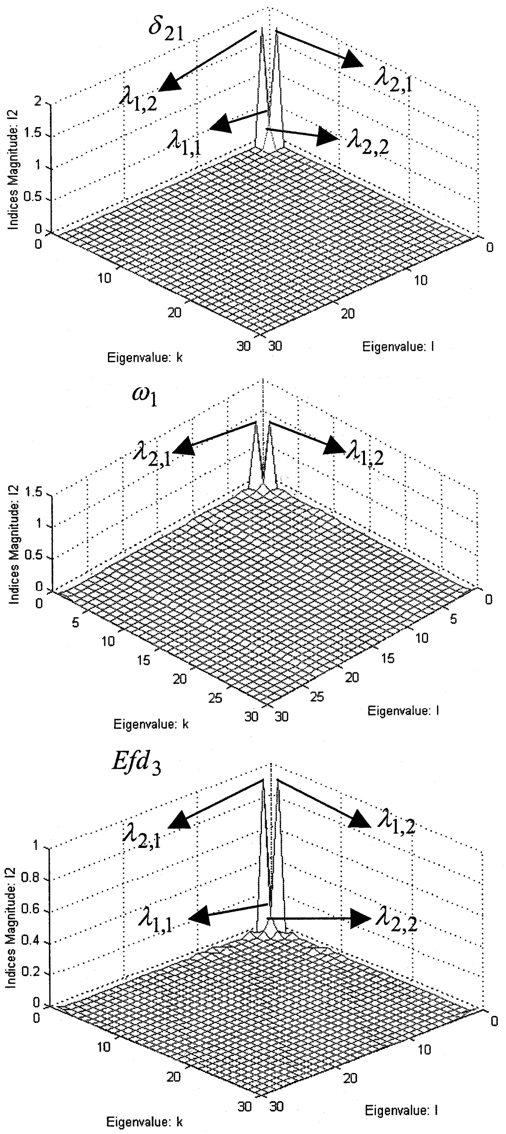

Fig. 4. Indices plots.

30 eigenvalues detectable from linear model, many interaction modes, like $\lambda_{i,j} = \lambda_i + \lambda_j$, also exist. We used the index $I2^i_{kl}$ (15) to compare, and as a measure for, the effects of these interaction modes in the time response and plotted it in three-dimensional coordinates. X and Y coordinates are used to denote k and l, and Z is used to show $I2^i_{kl}$. Please see the plot of $I2^i$ in Fig. 4. This figure shows that the effects of $\lambda_{1,2}$, $\lambda_{2,1}$, $\lambda_{1,1}$, $\lambda_{1,1}$ are dominant. These effects are discussed in the following subsection VI-A-7.

7) Analysis of the Differences between Nonlinear and Linear Simulation Results: Fig. 4 shows that there are considerable auto and cross interaction between inter-area modes, λ_1 and λ_2. On the other hand inspection of MI^i_j indices shows that generally zero mode causes quasiresonance condition. Therefore we conclude the following:

a) The interaction $\lambda_{1,2}$ and $\lambda_{2,1}$, ($\lambda_{1,2} = \lambda_{2,1} = \lambda_1 + \lambda_2 = -0.1444$), produces relatively large exponential term, $2\times\mathrm{real}(K^i_{1,2})e^{-0.1444t}$ in those states i, which have a considerably large index value $I2^i_{1,2}$ (or $I2^i_{2,1}$). This term makes the nonlinear system response differ from the linear modal simulation result. Therefore we must see an exponential decay in nonlinear simulation results compared with linear modal result. For example, please see δ_{2l} or ω_1 in Figs. 2 and 4.

b) $\lambda_{1,1}$ and $\lambda_{2,2}$ produce exponentially decaying sinusoidal term with frequency 1.1065 Hz, i.e., $2 \times \left|K^i_{1,1}\right| e^{-0.1444t} \cos\left(6.9548t + \angle K^i_{1,1}\right)$ in those states i which have considerably large index value $I2^i_{1,1}$ (or $I2^i_{2,2}$). This term also makes the nonlinear system response differ from the linear modal simulation result, i.e., we must see 1.1069 Hz oscillation frequency in states which have considerable interaction $\lambda_{1,1}$ and $\lambda_{2,2}$ while this frequency is not seen in linear modal results. For example please see δ_{2l} or E_{fd3} in Figs. 2 and 4.

c) The magnitude of MI^i_j for (1, 7, 2) and $(2,7,1) \in R'_2$ are ten times greater than other quasiresonance condition. These quasiresonance conditions produce, sinusoids with frequency of inter-area oscillation and with amplitudes that are time modulated exponentially decaying; $2\times \left|M^i_1\right| te^{0.0722t}\cos(3.4774t + \angle M^i_1)$. This term is added to the linear modal approximation term, and depending on its phase, we must see increase or decrease in the amplitude of the nonlinear simulation result with respect to linear modal simulation at frequency 0.5534 Hz. For example please see E_{fd3} in Fig. 2.

Simulation results show that if the damping of the inter-area mode is increased, nonlinearity effects become negligible and nonlinear system behaves as linear system.

B. 50-Generator, 145-Bus Power System

A 50-generator, 145-bus power system [11] is used to show the modal interaction phenomenon and the validity of modal series in simulating large power systems. Two axes model is used to model six generators that are highly influenced by fault and the classical model is used for other generators. This system has 155 eigenvalues with negative real part; 122 representing 61 complex conjugate pairs and 33 real eigenvalues. The frequencies of two damped oscillatory modes are 2.992 and 3.041 Hz and others are lying in the range, (0.003, 2.525) Hz.

For 0.9 second the line between buses 6 and 7 is opened and then closed to simulate a fault in the stressed system. Increasing the fault on time to 0.95 second made the system unstable. Fig. 5 shows considerable differences between linear modal and nonlinear simulation results, but shows negligible difference between second order modal series and nonlinear simulation.

The nonlinear system response and its DFT's show that there are some dominant oscillation frequencies, one of them is related to linear modes λ_{100}, $\lambda_{101} = -0.5275 \pm j(2\pi \times 1.2883)$ which is predictable from linear analysis, but the others are close to 2.5 Hz and are not predictable from linear analysis. Some of them are greater than 2.525 Hz and so are not in the range of linear mode frequencies. Inspection of $I2$ indices show that the dominant one of them, with frequency of 2.5766 Hz, is caused by $\lambda_{100,\,100}$ and $\lambda_{101,\,101}$. Also, $I1$ and $I2$ indicate that the dominant frequencies, 2.411 and 2.494 Hz, which are less than 2.525 Hz and thus in the range of linear modes are only

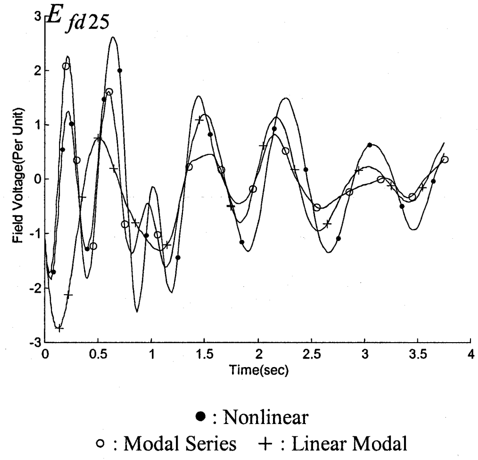

Fig. 5. Nonlinear, linear modal and second order modal series simulation results.

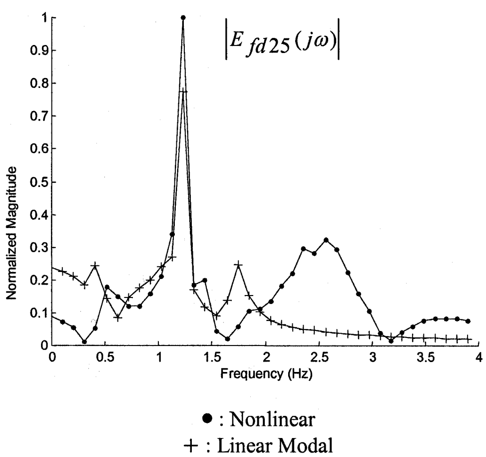

Fig. 6. Nonlinear and linear modal DFT's.

seen in nonlinear DFT's. They are caused by $\lambda_{104,\,104}$, $\lambda_{105,\,105}$, $\lambda_{100,\,104}$ and $\lambda_{101,\,105}$, where λ_{104} and λ_{105} are conjugate pairs, $-0.5941 \pm j(2\pi \times 1.2057)$ [7].

Comparing two DFT's indicates that there are some other tops in linear modal DFT's such as in frequency 1.7455 Hz, related to the linearly excited conjugate pairs λ_{74} and λ_{75}, $-0.2555 \pm j(2\pi \times 1.7455)$. These tops cannot be seen in nonlinear DFT's. Inspection of $I1$ indices showed that, those modes are relaxed more than ten times with respect to linear analysis by nonlinearity effects [7].

VII. Conclusion

The results presented in this paper validate that, there are considerable differences between nonlinear and linear modal simulation when the power system is stressed with the nonlinear modal simulations results more accurately representing the system behavior. The results also indicate that the newly defined selective indices can be used very effectively to explain the nature of these differences. Studies show three ways by which nonlinear interaction between linear modes make the response of nonlinear system differ from linear modal results; exponential decay, frequency combination and increase or decrease in amplitude.

Appendix

In this appendix modal series method is illustrated by a simple example. Let the solution of (A1) to the initial condition in some interval $[0, T)$ be (A2)

$$\dot{y} = \lambda y + \frac{1}{2}Hy^2 \tag{A1}$$

$$y(t) = F(t, y_0) \tag{A2}$$

By expanding this solution as a MacLaurin series with respect to y_0 one can find (A3), where $\alpha_i(t) = (\partial^i F/\partial t^i)|y_0 = 0$ and

$$\begin{aligned} f^i(t) =& \frac{\alpha_i(t)y_o^i}{i!} \\ y(t) =& \alpha_1 y_0 + \frac{1}{2}\alpha_2 y_0^2 + \frac{1}{6}\alpha_3 y_0^3 + \cdots \\ =& f^1(t) + f^2(t) + f^3(t) + \cdots \end{aligned} \tag{A3}$$

Suppose (A3) has a nonempty convergence domain φ for all $t \in [0, T)$. If one expands the solution of (A1) to the initial condition εy_0, where ε is arbitrary real number such that $\varepsilon y_0 \in \varphi$ then he finds (A4) and (A5)

$$\begin{aligned} y(t) =& F(t, \varepsilon y_0) \\ =& \alpha_1 \varepsilon y_0 + \frac{1}{2}\alpha_2 \varepsilon^2 y_0^2 + \frac{1}{6}\alpha_3 \varepsilon^3 y_0^3 + \cdots \\ =& \varepsilon f^1(t) + \varepsilon^2 f^2(t) + \varepsilon^3 f^3(t) + \cdots \end{aligned} \tag{A4}$$

$$y(0) = \varepsilon y_0 = \varepsilon f^1(0) + \varepsilon^2 f^2(0) + \varepsilon^3 f^3(0) + \cdots \tag{A5}$$

Equation (A4) must satisfy (A1) for any arbitrary ε, i.e.,

$$\begin{aligned} \varepsilon \dot{f}^1 + \varepsilon^2 \dot{f}^2 + \varepsilon^3 \dot{f}^3 + \cdots =& \varepsilon[\lambda f^1] + \\ & \varepsilon^2 \left[\lambda f^2 + \frac{1}{2}Hf^1 f^1\right] + \\ & \varepsilon^3 \left[\lambda f^3 + \frac{1}{6}H(f^1 f^2 + f^2 f^1)\right] + \\ & \vdots \end{aligned} \tag{A6}$$

therefore the coefficient of any order of ε on both sides of (A5) and (A6) must be equal, i.e.,

$$\begin{cases} \dot{f}^1 = \lambda f^1, & f^1(0) = y_0 \\ \dot{f}^2 = \lambda f^2 + 0.5Hf^1 f^1, & f^2(0) = 0 \\ \dot{f}^3 = \lambda f^3 + 0.5H(f^1 f^2 + f^2 f^1), & f^3(0) = 0 \\ \vdots, & \vdots \end{cases} \tag{A7}$$

The solution of (A7) can be found recursively using multi dimensional Laplace transform as (A8) and (A9). See equation

$$\begin{cases} f^1(s) = \frac{y_0}{(s-\lambda)} \\ f^2(s_1,s_2) = \frac{0.5Hy_0^2}{\{(s_1+s_2-\lambda)(s_1-\lambda)(s_2-\lambda)\}} \\ f^3(s_1,s_2,s_3) = \frac{0.5H^2y_0^3}{\{(s_1+s_2+s_3-\lambda)(s_1+s_2-\lambda)(s_1-\lambda)(s_2-\lambda)(s_3-\lambda)\}} \\ \vdots \end{cases} \tag{A8}$$

$$\begin{cases} f^1(t) = y_0e^{\lambda t} \\ f^2(t) = \frac{H}{2\lambda}y_0^2\{e^{2\lambda t} - e^{\lambda t}\} \\ f^3(t) = \frac{H^2}{4\lambda^2}y_0^3\{e^{3\lambda t} - 2e^{2\lambda t} + e^{\lambda t}\} \\ \vdots \end{cases} \tag{A9}$$

(A8) and (A9) at the top of the page.Therefore the solution of (A1) to the initial condition $y(0) = y_0$ is given by (A10). This is equal to the expansion of its analytic solution (A11)

$$\begin{aligned} y(t) =& f^1(t) + f^2(t) + f^3(t) + \cdots \\ =& y_0e^{\lambda t} + \frac{H}{2\lambda}y_0^2\left\{e^{2\lambda t} - e^{\lambda t}\right\} \\ &+ \frac{H^2}{4\lambda^2}y_0^3\left\{e^{3\lambda t} - 2e^{2\lambda t} + e^{\lambda t}\right\} + \cdots \end{aligned} \tag{A10}$$

$$\begin{aligned} y(t) =& \frac{1}{\left\{\frac{H}{2\lambda}y_0(1-e^{\lambda t}) + 1\right\}}y_0e^{\lambda t} \\ =& y_0e^{\lambda t}\left\{1 - \frac{H}{2\lambda}y_0(1-e^{\lambda t})\right. \\ &\left. + \frac{H^2}{4\lambda^2}y_0^2(1-e^{\lambda t})^2 + \cdots\right\} \\ =& \left\{y_0e^{\lambda t}\right\} + \left\{\frac{H}{2\lambda}y_0^2(e^{2\lambda t} - e^{\lambda t})\right\} \\ &+ \left\{\frac{H^2}{4\lambda^2}y_0^3(e^{3\lambda t} - 2e^{2\lambda t} + e^{\lambda t})\right\} + \cdots \end{aligned} \tag{A11}$$

REFERENCES

[1] V. Vittal, N. Bhatia, and A. A. Fouad, “Analysis of the inter-area mode phenomenon in power systems following large disturbances,” *IEEE Trans. Power Syst.*, vol. 6, pp. 1515–1521, Nov. 1991.

[2] Y. Tamura and N. Yorino, “Possibility of auto- & hetero -parametric resonances in power systems and their relationship with long-term dynamics,” *IEEE Trans. Power Syst.*, vol. PWRS-2, pp. 890–897, Nov. 1987.

[3] C. M. Lin, V. Vittal, W. Kliemann, and A. A. Fouad, “Investigation of modal interaction and its effects on control performance in stressed power systems using normal forms of vector felds,” *IEEE Trans. Power Syst.*, vol. 11, pp. 781–787, May 1996.

[4] G. Jang, V. Vittal, and W. Kliemann, “Effect of nonlinear modal interaction on control performance: Use of normal forms technique in control design, Part 1: General theory and procedure,” *IEEE Trans. Power Syst.*, vol. 13, pp. 401–407, May 1998.

[5] ——, “Effect of nonlinear modal interaction on control performance: Use of normal forms technique in control design, Part 2: Case studies,” *IEEE Trans. Power Syst.*, vol. 13, pp. 408–413, May 1998.

[6] J. Thapar, V. Vittal, W. Kliemann, and A. A. Fouad, “Application of the normal form of vector fields to predict inter-area separation in power systems,” *IEEE Trans. Power Syst.*, vol. 12, pp. 844–850, May 1997.

[7] N. Pariz, “Analysis of Nonlinear System Behavior; the Case of Stressed Power Systems,” Ph.D. dissertation, Department of Electrical Engineering, Ferdowsi University, Mashhad, Iran, Sept. 2001.

[8] N. Pariz, H. M. Shanechi, and E. Vaahedi, “Extended modal series method for explaining nonlinear system behavior and its application in stressed power systems,” *J. Eng.*, vol. 13, no. 1, 2001–2.

[9] S. K. Starrett and A. A. Fouad, “Nonlinear measures of mode-machine participation,” *IEEE Trans. Power Syst.*, vol. 13, pp. 389–394, May 1998.

[10] P. Kundur, *Power System Stability and Control*. New York: McGraw-Hill, 1993.

[11] V. Vittal, “Transient stability test systems for direct stability methods,” *IEEE Comment Rep., Trans. Power Syst.*, vol. 7, no. 1, February 1992.

Naser Pariz received the B.Sc. and M.Sc. degrees in electrical engineering with honors from the Ferdowsi University of Mashhad, Mashhad, Iran, in 1988 and 1991, respectively. He received the Ph.D. degree from the Department of Electrical Engineering at Ferdowsi University in 2001.

He was a Lecturer at Ferdowsi University from 1991 to 1995, where he is now assistant professor. His research interests are power and control systems.

Hasan Modir Shanechi (SM’85) received the M.Sc. degree in electrical engineering with distinction from Tehran University, Iran, and the Ph.D. degree in system science from Michigan State University, East Lansing.

He has been with New Mexixo Tech, Socorro, NM, since 2001. Prior to that, he had been with the Electrical Engineering Department of Ferdowsi University for 20 years. His research interests include power system operation, economics, and dynamics, large scale and intelligent systems, and distributed energy resources.

Ebrahim Vaahedi (F’99) received the M.Sc. and Ph.D. degrees from Imperial College, London, U.K., in 1976 and 1979, respectively.

Currently, he is a Senior Manager at Perot Systems, Dallas, TX, where he has been engaged in the development of Grid Operation and Market Operation Systems and other energy related consulting services.